Analysis of composition and microstructural uniformity of hybrid glass/carbon fibre composites

Beauson, Justine; Markussen, Christen Malte; Madsen, Bo

Published in:
Proceedings of the Risø International Symposium on Materials Science

Publication date:
2013

Document Version
Publisher's PDF, also known as Version of record

Proceedings of the 34th Risø International Symposium on Materials Science:
Processing of fibre composites – challenges for maximum materials performance
Editors: B. Madsen, H. Lilholt, Y. Kusano, S. Fæster and B. Ralph
Department of Wind Energy, Risø Campus
Technical University of Denmark, 2013

ANALYSIS OF COMPOSITION AND MICROSTRUCTURAL UNIFORMITY OF HYBRID GLASS/CARBON FIBRE COMPOSITES

Justine Beauson, Christen Malte Markussen and Bo Madsen

Composites and Materials Mechanics, Department of Wind Energy,
Risø Campus, Technical University of Denmark,
DK-4000 Roskilde, Denmark

ABSTRACT

In hybrid fibre composites, the intermixing of the two types of fibres imposes challenges to obtain materials with a well-defined and uniform microstructure. In the present paper, the composition and the microstructural uniformity of hybrid glass/carbon fibre composites mixed at the fibre bundle level are investigated. The different levels of compositions in the composites are defined and experimentally determined. The composite volume fractions are determined using an image analysis based procedure. The global fibre volume fractions are determined using a gravimetrical based method. The local fibre volume fractions are determined using volumetric calculations. A model is presented to predict the interrelation of volume fractions in hybrid fibre composites. The microstructural uniformity of the composites is analysed by the determined variation in composite volume fractions. Two analytical methods, a standard deviation based method and a fast Fourier transform method, are used to quantify the difference in microstructural uniformity between composites, and to detect and quantify any repeating pattern in the composite microstructure.

1. INTRODUCTION

Hybrid fibre composites consisting of two types of fibres (e.g. glass and carbon fibres) are attracting scientific and industrial interest due to the potential synergistic effect of having reinforcement fibres with different properties. The so-called “hybrid effect” is explored on a mechanical basis (e.g. to have longer fatigue life, and larger compression strength), and, equally important, it is explored for economic reasons to improve the materials cost-performance. Earlier work has addressed hybrid fibre composites by analysing the difference in failure strain and dimensions between the two reinforcement fibres with respect to improved composite strength (Aveston and Kelly 1980). Later on, in the 1990’ies, within an EU Framework Programme (JOULE) with participation from Risø National Laboratory, Denmark, studies were performed on the manufacturing and testing of hybrid composites for wind turbine rotor blades.

Recently, the hybrid fibre concept has been addressed in a number scientific studies (e.g. Hermann et al. 2006, Hillermeier 2009, Zhang et al. 2012), forming also a central element in a current Danish technology project (Blade King).

By their nature, composites are heterogeneous materials due to the dispersion of discrete fibres in a continuous matrix. For conventional composites consisting of a single type of fibres, fibre/matrix preforms and composite manufacturing techniques have been developed to produce materials with a well-defined and uniform microstructure. Hence, this allows for the use of representative geometrical models of the microstructure (so-called representative volume elements) for the analysis and modelling of the (mechanical) properties of the composites. This supports the use of composites in highly demanding structural applications, such as rotor blades for wind turbines. However, in the case of hybrid fibre composites consisting of two fibre types, the intermixing of the two fibres will impose challenges to obtain a similar high degree of microstructural uniformity to allow reliable analysis and modelling of properties. Different fibre intermixing levels can be defined: fibre-fibre, bundle-bundle and ply-ply, and each level bring forward specific microstructural characteristics.

In the present paper, based on experimental data from a number of manufactured hybrid glass/carbon fibre composites, the microstructure of the composites is studied by two aspects. The first one is related to the composition of the composites, i.e. volume fractions of the two composite phases, the two fibre types and the matrix, and with focus on establishing a model for their interrelations. The second one is related to the microstructural uniformity of the composites, and with focus on the variation in volume fractions of the two composite phases.

2. MATERIALS AND METHODS

Plates of hybrid and non-hybrid fibre composites were made with the same type of glass fibre roving (Hybon2026 - PPG FibreGlass, 2447 tex) and the same type of carbon fibre roving (PANEX35 - Zoltek, 3645 tex). One type of preform was used, uniaxial fibre assemblies made by filament-winding, and with variable number of glass and carbon rovings to have composites with different composition and microstructure. The composite plates were made with vacuum infusion using epoxy (DowAirstone) as matrix, and the plates had dimensions of 450 mm x 475 mm x thickness of the plate (see Table 1). Fig. 1 shows the cross section of the eight manufactured composite plates, and Table 1 summarizes their specifications. In the table, β is the hybrid fibre *weight* mixing ratio:

$$\beta = \frac{m_{f\,carbon}}{m_{f\,carbon} + m_{f\,glass}} \tag{1}$$

where m_f is the mass of fibres. Likewise, a hybrid fibre *volume* mixing ratio γ can be defined, and the relation between β and γ can be established:

$$\gamma = \frac{v_{f\,carbon}}{v_{f\,carbon} + v_{f\,glass}} \tag{2}$$

$$\gamma = \frac{\rho_{f\,glass} \cdot \beta}{\rho_{f\,glass} \cdot \beta + \rho_{f\,carbon}\,(1-\beta)} \tag{3}$$

where v_f is the volume of fibres, and ρ_f is the density of fibres. The calculated values of γ shown in Table 1 are based on a glass fibre density of 2.58 g/cm^3, and a carbon fibre density of 1.83 g/cm^3, which were measured by pycnometry.

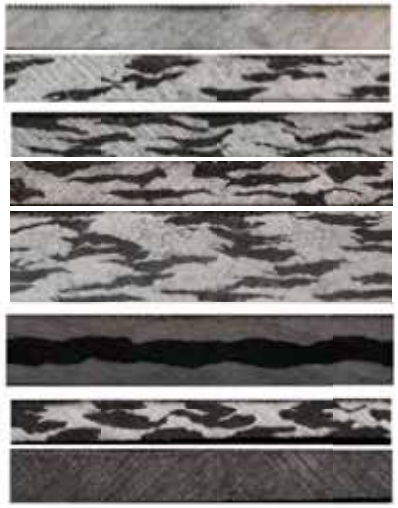

Fig. 1. Cross sections of the hybrid and non-hybrid glass/carbon fibre composites.

Table 1. Specifications of the manufactured hybrid and non-hybrid glass/carbon fibre composites.

Composite plate code	Number of preform layers	Plate thickness [mm]	Hybrid fibre weight mixing ratio, β	Hybrid fibre volume mixing ratio, γ
CXG-01	10	3.0	0.00	0.00
CXG-06	3	3.4	0.21	0.27
CXG-03	3	3.1	0.28	0.35
CXG-02	3	3.2	0.28	0.35
CXG-07	6	5.8	0.28	0.35
CXG-10	6	6.1	0.28	0.35
CXG-05	4	3.1	0.44	0.53
CXG-04	6	3.5	1.00	1.00

2.1 Determination of composition. In the present paper, three levels of compositions in the hybrid fibre composites are defined and determined. In Fig. 2a, a hybrid composite composed of glass and carbon fibres is schematically represented, and used to illustrate the definitions:

- *Composite volume fraction* V_c, which is exemplified in Fig. 2b with the volume of the carbon fibre composite region in black, in relation to the total volume of the hybrid composite framed in red. V_c will be assessed by an image analysis procedure.
- *Global fibre volume fractions* V_f, which is exemplified in Fig. 2c with the volume of the carbon fibres in black in relation to the total volume of the hybrid composite framed in red. V_f will be measured with the conventionally applied gravimetrical based method.
- *Local fibre volume fractions* V_f^*, which is exemplified in Fig. 2d with the volume of the carbon fibres in black in relation to the volume of the carbon fibre composite framed in red. V_f^* will be calculated with Eq. (7) detailed hereafter.

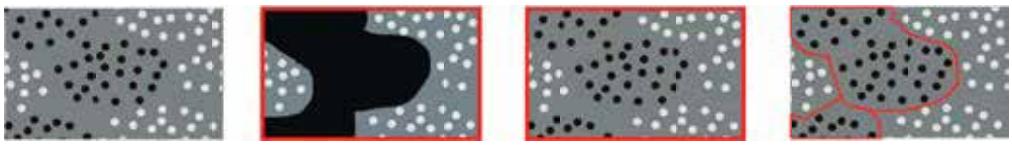

a) b) c) d)

Fig. 2. The three levels of compositions in hybrid fibre composites: a) general view of hybrid composite with glass fibres (white) and carbon fibres (black) in a common matrix (grey), b) composite volume fraction, c) global fibre volume fraction, and d) local fibre volume fraction. The volumes (or areas) framed in red indicate the reference volumes. The three compositions are exemplified by the carbon fibres.

The definitions of the above-mentioned three levels of compositions in hybrid composites, and their relationship are given here (exemplified by carbon fibres):

$$V_{c\,carbon} = \frac{v_{c\,carbon}}{v_{c\,carbon} + v_{c\,glass}} \quad \text{(composite volume fraction)} \tag{4}$$

$$V_{f\,carbon} = \frac{v_{f\,carbon}}{v_{f\,carbon} + v_{f\,glass} + v_{matrix}} \quad \text{(global fibre volume fraction)} \tag{5}$$

$$V^{*}_{f\,carbon} = \frac{v_{f\,carbon}}{v_{f\,carbon} + v^{*}_{matrix}} \quad \text{(local fibre volume fraction)} \tag{6}$$

$$V_{f\,carbon} = V^{*}_{f\,carbon} \cdot V_{c\,carbon} \tag{7}$$

where the asterisk (*) defines the local non-hybrid composite region in the hybrid fibre composite (see Fig. 2d). In these definitions, the porosity content in the composites is assumed to be zero.

Here follows descriptions of the experimental methods used to determine V_c and V_f in the manufactured hybrid fibre composites.

To determine the composite volume fractions (V_c), samples with widths in the range 20 - 50 mm, transverse to the fibre direction, were cut from the composite plates, and the cross sections were grinded and polished in several steps in order to get a smooth surface.

Grayscale images of the samples were taken using an optical microscope with a motorized XY stage. The software *DeltaPix* was used to calculate how many images were needed to cover the cross sectional area of the samples, and the stage was automatically moved by the software. In addition, the stitching of the captured images was performed automatically by the software.

The grayscale images were then prepared for image analysis with the procedure illustrated in Fig. 3. The grayscale image of the hybrid composite, as exemplified in Fig. 3a, is composed of dark grey regions which are the carbon fibre composite phase, and light grey regions which are the glass fibre composite phase. The first step in the procedure is to adjust the contrast, see Fig. 3b. Then, the regions of glass fibre composite are selected using the *Quick selection tool* in *Adobe Photoshop*. This tool is an interactive segmentation tool, which will partition the image based on user provided input, texture information (colours) and/or edge information (contrast). In the *Quick selection tool,* the users input is provided through a brush stroke tool that enables in the present case to select the glass fibre composite regions, see Fig. 3c. Finally, the contrast is adjusted to get a binary image, see Fig. 3d. An example is given in Fig. 4 with the composite

plate CXG-07.

In the obtained binary images, the number of pixels having a value of 1 was counted using a routine in *Mathematica*. This number is divided with the total number of pixels in the image to give *area fractions*, which are assumed to be equal to *volume fractions*, because of the uniaxial nature of the composites, i.e. it is assumed that each observed unit in the transverse cross section is extending continuously in the longitudinal direction.

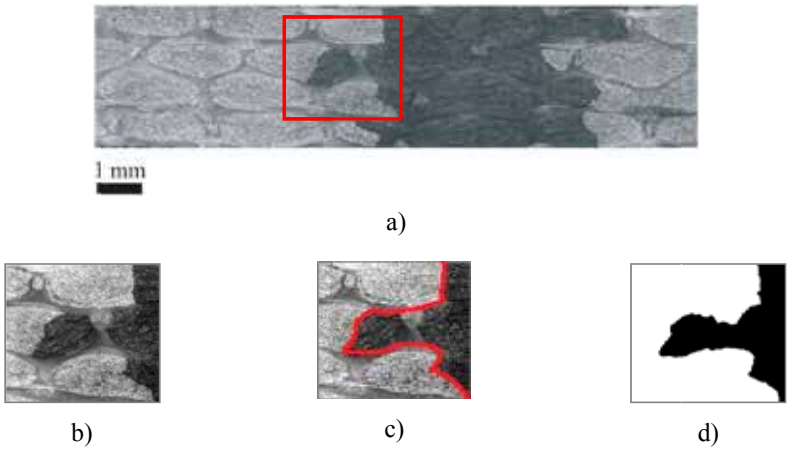

Fig. 3. Image preparation: a) original grayscale image of hybrid fibre composite, where the red box shows: b) the adjustment in contrast, c) the selection process with *Photoshop*, and d) the final binary image.

Fig. 4. Hybrid glass/carbon fibre composite with β = 0.28 and γ = 0.35 (CXG-07): original grayscale image (top), and resulting binary image (bottom).

The global fibre volume fractions (V_f) in the composites were determined using a gravimetrical based method. This method consists of weighing of samples in successive steps. The composite samples are first dried and weighed in air. Then, the samples are sealed and weighed in water. The epoxy matrix is then removed by burning at 450 °C in a nitrogen environment. The resulting assembly of carbon and glass fibres are weighed. Finally, the carbon fibres are removed by burning at 625 °C in air, and the remaining glass fibres are weighed.

Finally, the local fibre volume fractions (V_f^*) in the composites were calculated using Eq. (7) with the experimentally determined values of V_c and V_f.

In principle, the local fibre volume fractions could also be determined directly by image analysis. However, this method presents one major difficulty, which is the selection of

representative local areas. Fig. 5 shows examples of three selected areas in a glass fibre composite region. The local glass fibre volume fractions are found to vary from about 0.40 to 0.60.

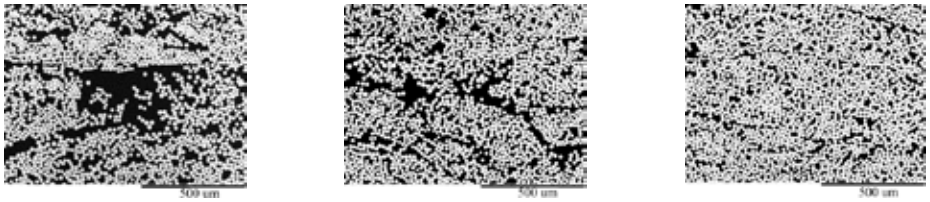

a) $V^*_{f\,glass} = 0.42$ b) $V^*_{f\,glass} = 0.54$ c) $V^*_{f\,glass} = 0.63$

Fig. 5. Examples of determined local glass fibre volume fractions in three areas of a glass fibre composite region.

2.2. Determination of microstructural uniformity. As indicated by the images in Fig. 1, the composition of the hybrid fibre composites will be varying depending on the location and size of the selected cross sectional area. As an example, the composite CXG-06 shows large areas of glass composite rich regions, which means that at certain cross sectional areas of the composite, the glass fibre composite volume fraction is very high (approaching 1.0).

To describe the variation in composition of the composites, V_c is determined in rectangular cross sectional areas, i.e. windows, with a width of 0.1 mm, and with a height equal to the height of the image, i.e. from one edge to the other edge of the sample. V_c is determined in windows successively moved from one end (left side) to the other end (right side) of the image. This result in a curve showing V_c as a function of the position across the sample (see example in Fig. 10).

In order to quantify the microstructural uniformity of the composites, the determined variation in V_c is then analysed using two different methods: *a standard deviation based method*, and *a fast Fourier transform method.* The two methods will be explained in details later on.

3. COMPOSITION OF HYBRID COMPOSITES

3.1. Composite volume fractions and global fibre volume fractions. The obtained binary images of the hybrid glass/carbon fibre composites are shown in Fig. 6, and the determined values of V_c and V_f are summarized in Table 2.

Table 2. Determined composite volume fractions and global fibre volume fractions in the manufactured hybrid and non-hybrid glass/carbon fibre composites.

Composite plate code	β	$V_{c\,carbon}$	$V_{c\,glass}$	$V_{f\,carbon}$	$V_{f\,glass}$
CXG-01	0.00	0.00	1.00	0.00	0.59
CXG-06	0.21	0.30	0.70	0.15	0.41
CXG-03	0.28	0.36	0.64	0.20	0.38
CXG-02	0.28	0.35	0.65	0.20	0.37
CXG-07	0.28	0.39	0.61	0.21	0.38
CXG-10	0.28	0.39	0.61	0.21	0.38
CXG-05	0.44	0.54	0.46	0.28	0.31
CXG-04	1.00	1.00	0.00	0.53	0.00

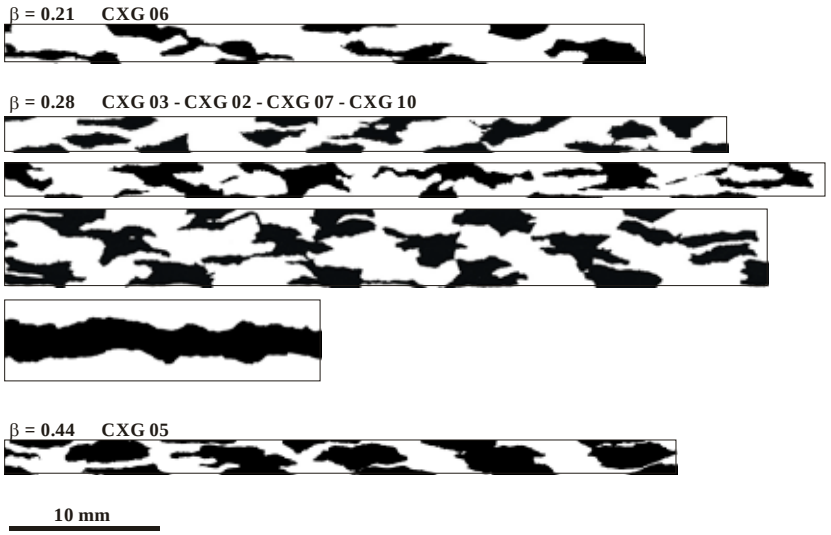

Fig. 6. Binary images of the hybrid glass/carbon fibre composites.

The variation in the results due to the sensitivity of the applied image analysis procedure was tested. The main source of error in the procedure to determine V_c comes from the objectivity of the operator when the *Quick selection tool* is used to manually detect the border between the two composite regions. This effect was tested by repeating three times the procedure on the same image. The results are shown in Fig. 7, and it can be observed that the difference between the determined values of V_c is negligible.

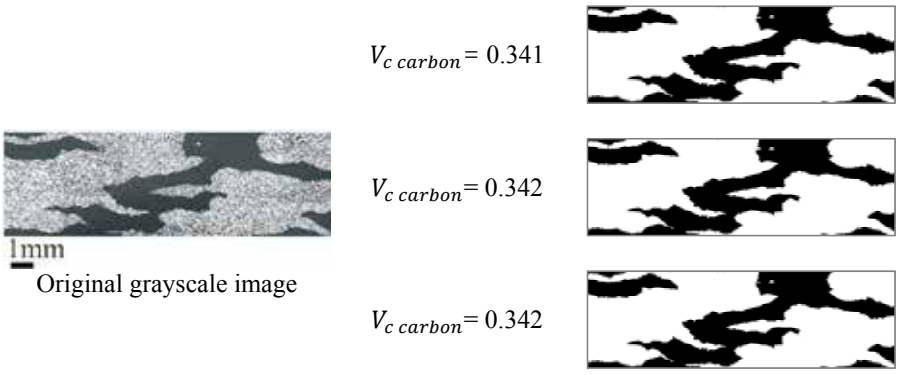

Fig. 7. Results obtained for the sensitivity testing of the image analysis procedure. The procedure was repeated three times on the same image to determine V_c.

3.2. Local fibre volume fractions. From Eq. (7), the local carbon and glass fibre volume fractions, $V^*_{f\,carbon}$ and $V^*_{f\,glass}$ are calculated based on the experimental data in Table 2. The results are summarized in Table 3.

Table 3. Calculated local glass and carbon fibre volume fraction in the manufactured hybrid glass/carbon fibre composites.

Composite plate code	$\boldsymbol{V^*_{f\,carbon}}$	$\boldsymbol{V^*_{f\,glass}}$
CXG-06	0.50	0.59
CXG-03	0.56	0.59
CXG-02	0.57	0.57
CXG-07	0.54	0.62
CXG-10	0.54	0.62
CXG-05	0.56	0.62
Average	**0.54**	**0.60**

It can be realized that the fibre volume fractions determined with the gravimetric method for the non-hybrid composites, CXG-04, containing only carbon fibres, and CXG-01, containing only glass fibres (see Table 2), can be compared to the calculated local carbon and glass fibre volume fractions in the hybrid composites.

The fibre volume fraction of CXG-04 is 0.53, and this compares well to the mean value on 0.54 for the calculated local carbon fibre volume fractions. Similarly, the fibre volume fraction of CXG-01 is 0.59 and this compares well to the mean value on 0.60 for the calculated local glass fibre volume fractions.

Thus, the local fibre volume fractions in the hybrid composites can be closely approximated by the fibre volume fractions determined in the related non-hybrid composites. In other words, it is demonstrated that the values of the local fibre volume fractions in hybrid composites can be determined a priori by manufacturing of the two non-hybrid fibre composites, and by determining the fibre volume fractions in these composites.

4. MODEL FOR COMPOSITION OF HYBRID COMPOSITES

Hereafter follows the derivation of model equations for the interrelation of volume fractions in hybrid composites. The equations can be used to calculate the global fibre volume fractions (V_f) and composite volume fractions (V_c) as a function of the hybrid fibre volume mixing ratio (γ), and with the local fibre volume fractions (V_f^*) as input parameters.

To derive the model equations, some useful support equations can be established on beforehand:

- $\gamma = \frac{v_{f\,carbon}}{v_{f\,carbon} + v_{f\,glass}} = \frac{1}{\frac{v_{f\,glass}}{v_{f\,carbon}} + 1}$
- $\frac{v_{f\,glass}}{v_{f\,carbon}} = \frac{1}{\gamma} - 1 = \frac{1-\gamma}{\gamma}$
- $1 - \gamma = 1 - \frac{v_{f\,carbon}}{v_{f\,carbon} + v_{f\,glass}} = \frac{v_{f\,glass}}{v_{f\,carbon} + v_{f\,glass}}$

The equation for the *global carbon fibre volume fraction* is derived as follows:

$$V_{f\,carbon} = \frac{v_{f\,carbon}}{v_c} = \frac{v_{f\,carbon}}{v_{c\,glass} + v_{c\,carbon}} = \frac{1}{\frac{v_{c\,glass}}{v_{f\,carbon}} + \frac{v_{c\,carbon}}{v_{f\,carbon}}} = \frac{1}{\frac{v_{f\,glass}}{V^*_{f\,glass}} \cdot \frac{1}{v_{f\,carbon}} + \frac{1}{V^*_{f\,carbon}}}$$

$$V_{f\,carbon} = \frac{1}{\frac{1}{V^*_{f\,glass}} \cdot \frac{1-\gamma}{\gamma} + \frac{1}{V^*_{f\,carbon}}} \tag{8}$$

The equation for the *global glass fibre volume fraction* is derived in the same way:

$$V_{f\,glass} = \frac{v_{f\,glass}}{v_c} = \frac{v_{f\,glass}}{v_{c\,glass} + v_{c\,carbon}} = \frac{1}{\frac{v_{c\,glass}}{v_{f\,glass}} + \frac{v_{c\,carbon}}{v_{f\,glass}}} = \frac{1}{\frac{1}{V^*_{f\,glass}} + \frac{v_{f\,carbon}}{V^*_{f\,carbon}} \cdot \frac{1}{v_{f\,glass}}}$$

$$V_{f\,glass} = \frac{1}{\frac{1}{V^*_{f\,glass}} + \frac{1}{V^*_{f\,carbon}} \cdot \frac{\gamma}{1-\gamma}} \tag{9}$$

The porosity content is assumed to be 0, and the *global matrix volume fraction* is therefore calculated as follows:

$$V_{matrix} = 1 - V_{f\,carbon} - V_{f\,glass} \tag{10}$$

The equations for the *carbon and glass composite volume fractions* are derived as follows:

$$V_{c\,carbon} = \frac{v_{c\,carbon}}{v_c} = \frac{v_{c\,carbon}}{v_{c\,glass} + v_{c\,carbon}} = \frac{1}{\frac{v_{c\,glass}}{v_{c\,carbon}} + 1} = \frac{1}{1 + \frac{v_{f\,glass}}{V^*_{f\,glass}} \cdot \frac{V^*_{f\,carbon}}{v_{f\,carbon}}}$$

$$V_{c\,carbon} = \frac{1}{1 + \frac{V^*_{f\,carbon}}{V^*_{f\,glass}} \cdot \frac{1-\gamma}{\gamma}} \tag{11}$$

$$V_{c\,glass} = \frac{v_{c\,glass}}{v_c} = \frac{v_{c\,glass}}{v_{c\,glass} + v_{c\,carbon}} = \frac{1}{1 + \frac{v_{c\,carbon}}{v_{c\,glass}}} = \frac{1}{1 + \frac{v_{f\,carbon}}{V^*_{f\,carbon}} \cdot \frac{V^*_{f\,glass}}{v_{f\,glass}}}$$

$$V_{c\,glass} = \frac{1}{1 + \frac{V^*_{f\,glass}}{V^*_{f\,carbon}} \cdot \frac{\gamma}{1-\gamma}} \tag{12}$$

In the equations (8) - (12), γ is used as the independent variable. It is however more appropriate to use β as the independent variable, since the two fibre types most typically is mixed by their weights in the hybrid fibre preforms. Thus, β is typically accurately controlled, and known for a given preform. The relation between γ and β is given by Eq. (3).

In Figs. 8 and 9, the model equations (8) – (12) are plotted for the hybrid glass/carbon fibre composites. The used values of local carbon and glass fibre volume fractions are 0.53 and 0.59, respectively, which are the values determined from the non-hybrid composites (CXG-04 and CXG-01). The experimental data of the hybrid composites (Table 2) is shown together with the model lines.

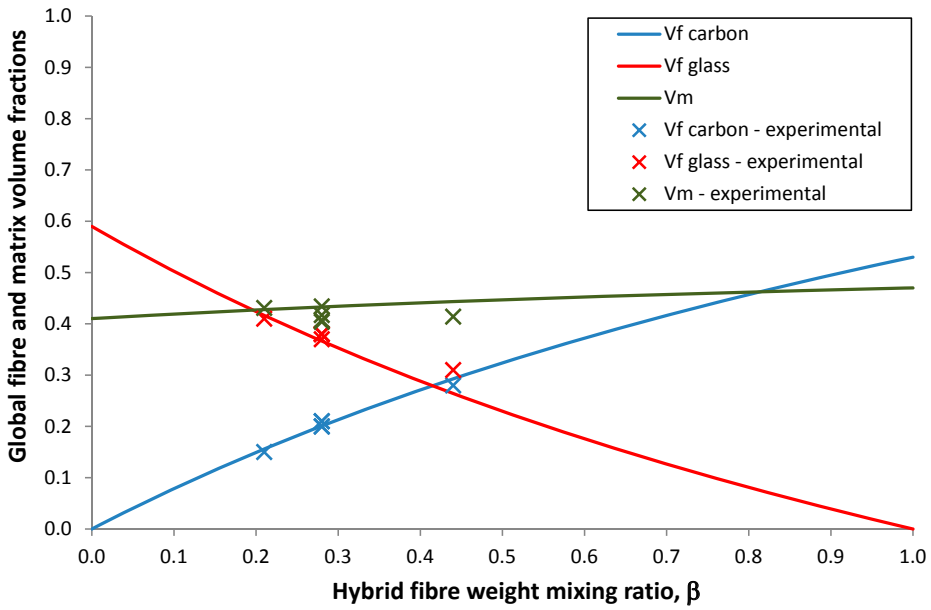

Fig. 8. Global fibre and matrix volume fractions in hybrid glass/carbon fibre composites as function of the hybrid fibre weight mixing ratio (β), model predictions and experimental data.

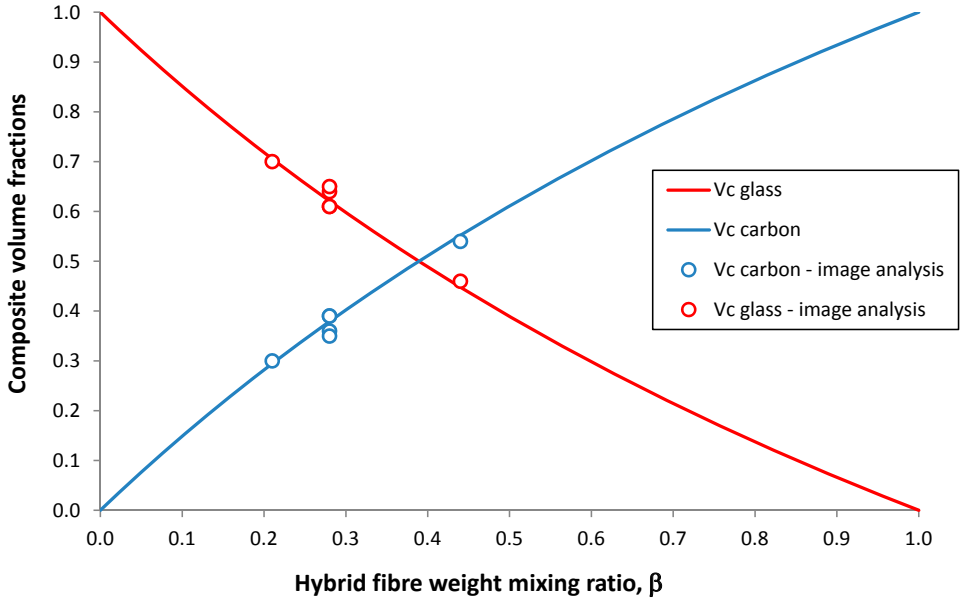

Fig. 9. Composite volume fractions in hybrid glass/carbon fibre composites as function of the hybrid fibre weight mixing ratio (β), model predictions and experimental data.

As can be observed in Figs. 8 and 9, there is generally a good agreement between the model lines, and the experimental data points. Thus, it is demonstrated that *the model equations are useful for the prediction of the composition in hybrid fibre composites, and thereby for the design of hybrid composites with wanted property profiles*.

5. MICROSTRUCTURAL UNIFORMITY OF HYBRID COMPOSITES

For the analysis of the microstructural uniformity, the two composites CXG-05 and CXG-10 were selected since they have a marked difference in their microstructure (see Fig. 6). CXG-05 has a *bundle-bundle* structure, and CXG-10 has a *ply-ply* structure. The image of CXG-10 is about half the width of the image of CXG-05 (about 20 vs. 40 mm), and it was therefore prolonged by stitching together twice the same image.

The first step in the quantification of the microstructural uniformity is to present the variation in the composite composition from one end of the composite sample to the other.

The results of the determined $V_{c\ glass}$ for every 0.1 mm of the two composites are shown in Fig. 10, where the composition is plotted against the position across the sample (or image). The dashed straight lines in Fig. 10 show the average $V_{c\ glass}$ values (which are similar to the ones in Table 2):

$$V_{c\ glass\ bundle-bundle} = 0.46 \quad \text{and} \quad V_{c\ glass\ ply-ply} = 0.61$$

The bundle-bundle curve is oscillating from about 0.2 to about 0.8, and the ply-ply curve is oscillating from about 0.5 to about 0.7. In each case, the difference between the two extreme values gives an indication of the dispersion of $V_{c\ glass}$, which reflects how constant the composition is across the composite. It is therefore clear that the ply-ply composite has a roughly constant composition compared to the bundle-bundle composite.

Other indications given in Fig. 10 for the bundle-bundle composite are the presences of glass composite rich regions ($V_{c\ glass} > 0.8$) and carbon composite rich regions ($V_{c\ glass} < 0.2$). The distance between these consecutive regions can roughly be estimated to 4 mm. Thus, one can say that the bundle-bundle composite is varying between two very different composite compositions within few millimetres across the sample.

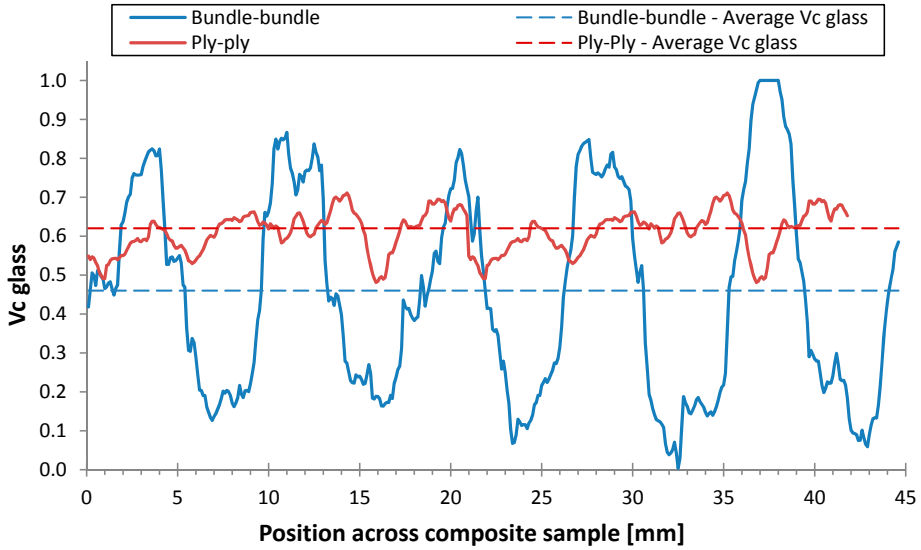

Fig. 10. Glass composite volume fraction ($V_{c\ glass}$) as function of position across the composite sample for composites with a bundle-bundle structure (CXG-05) and with a ply-ply structure (CXG-10). Shown are also average values.

In order to analyse the observed variation in V_c, and thereby to be able to quantify the microstructural uniformity, two methods are presented.

It can be realized that the variation in the determined values of V_c (see Fig. 10) depends on the width of the cross sectional windows used to determine V_c. It can be expected that the smaller the width of the cross sectional windows, the larger the variation of the determined values of V_c. This qualitative expectation will be quantified by *a standard deviation based method*, where a parameter D is calculated for a given width of the cross sectional windows (k) to represent the deviation in V_c from the overall (true) value of V_c.

$$D(k) = \sqrt{\frac{\sum_{i=1}^{n}\left(X_i - \bar{X}\right)^2}{n-1}} \tag{13}$$

where X_i are the determined values of V_c for all possible locations of a cross sectional window with a width of k (in mm) across the composite sample, $\bar{X}$ is the overall V_c determined for the entire sample (or image), i.e. $\bar{X}$ is equal to the average values shown in Fig. 10. The parameter n is the number of all possible locations of a cross sectional window with a width of k across the composite sample (or image). The parameter D is named *characteristic deviation* to designate that the parameter is not used in the normal statistical meaning of a standard deviation.

The parameter k and the width of the composite sample (or image) have to be a multiple of 0.1 mm, and the parameter n can then be calculated:

$$n = \textit{width of composite sample} \cdot 10 - k \cdot 10 + 1 \tag{14}$$

The presented method can be exemplified on the image in Fig. 6 of the hybrid composite with

the bundle-bundle structure (CXG-05), where the width of the image is 44.5 mm, and the overall V_c for the glass fibre composite phase is determined to be 0.46.

- For a cross sectional window width of 0.1 mm (k = 0.1 mm), there will be n = 445 possible locations of the window. On each of these n locations, V_c is determined, and then D is calculated by Eq. (13) to be 0.27. Thus, for a window width of 0.1 mm, the characteristic deviation of V_c can be stated to be 0.46 ± 0.27.
- For a cross sectional window width of 4.0 mm (k = 4.0 mm), there will be n = 406 possible locations of the window. On each of these n locations, V_c is determined, and then D is calculated by Eq. (13) to be 0.18. Thus, for a window width of 4.0 mm, the characteristic deviation of V_c can be stated to be 0.46 ± 0.18.

By varying k stepwise from the minimum window width (= 0.1 mm) to the maximum window width (= width of the image – 0.1mm, where n = 2), a curve can be established showing D as a function of k.

In Fig. 11, the curves for D as a function of k are shown for the bundle-bundle composite and the ply-ply composite (CXG05 and CXG10). Firstly, it can be observed that the deviations in V_c are smaller for the ply-ply composite. As an example, for a window width of 4 mm, the characteristic deviations of V_c are 0.46 ± 0.18 and 0.61 ± 0.02 for the bundle-bundle composite and the ply-ply composite, respectively. Accordingly, V_c will therefore vary from about 0.28 to 0.64 for the bundle-bundle composite depending on the location of the 4 mm cross sectional window, whereas V_c will only vary from about 0.59 to 0.63 for the ply-ply composite.

From this first observation, one can say that the presented method is able *to quantify the difference in microstructural uniformity between composites*.

Secondly, it can be observed in Fig. 11 that for the bundle-bundle composite, the curve is clearly oscillating, whereas for the ply-ply composite, the curve is more flat. This indicates that the bundle-bundle composite contain a repeating pattern in the microstructure, whereas the ply-ply composite does not contain such a pattern.

In Fig. 11, the bundle-bundle curve shows a first minimum at a width of 8.9 mm, and the following minimum values are roughly at a multiple of this value, located at 17.1 mm and 25.7 mm. These values are easily and precisely determined. Thus, at every about 9 mm, the composition of the composite has gone through a glass composite rich region, and a carbon composite rich region. The same observation can be made from the results in Fig. 10. It can be realised that for samples with widths equal to a multiple of the width of the repeating pattern, the variation in V_c is at a minimum. In contrast, for samples with widths equal to a multiple of half the width of the repeating pattern, the variation in V_c is at a maximum.

From this second observation, one can say that the presented method is able *to detect and quantify any repeating pattern in the microstructure of composites.*

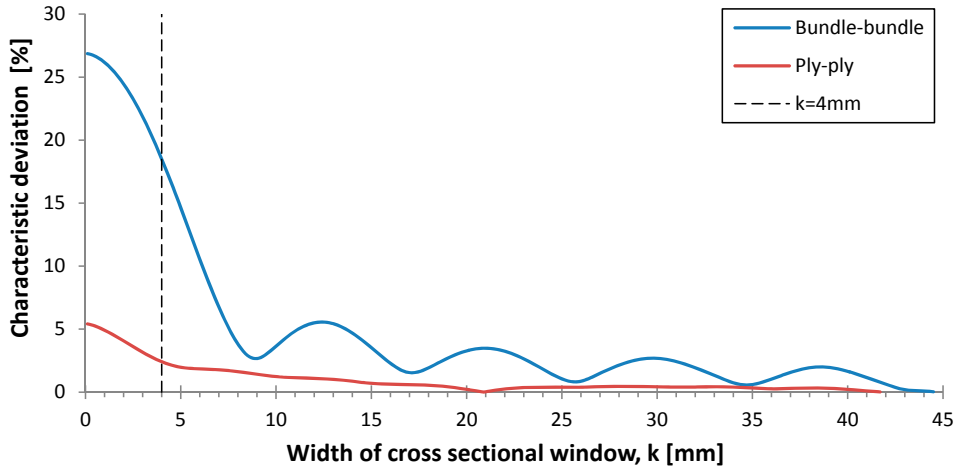

Fig. 11. Characteristic deviation of V_c as a function of width of the cross sectional window, obtained by the standard deviation based method. Results are shown for a composite with a bundle-bundle structure, and for a composite with a ply-ply structure.

In order to analyse further the observed variation behaviour in Fig. 10, a second method was used, a *fast Fourier transform method*. For that method, the two curves in Fig. 10 were considered as oscillating signals from which fundamental frequencies could be determined, and the Fourier transforms were calculated using the fast Fourier transform function in *Excel.*

The results obtained by this method are presented in Fig. 12, and show the frequency magnitude as a function of frequency range. It can be observed that the bundle-bundle curve shows a clear first peak at a frequency of 0.117 mm^{-1}, which correspond to a period of 8.5 mm. The ply-ply curve does not show any noteworthy peak. The period found for the bundle-bundle curve corresponds well to the results obtained by the standard deviation based method.

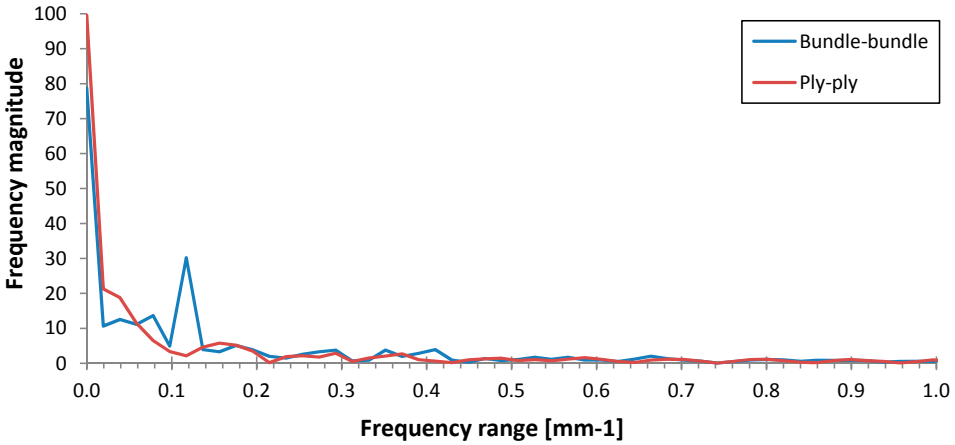

Fig. 12. Frequency magnitude as a function of frequency range obtained by the fast Fourier transform method. Results are shown for a composite with a bundle-bundle structure, and for a composite with a ply-ply structure.

6. CONCLUSIONS

The three levels of compositions in hybrid fibre composites were defined, experimentally determined and analysed. A model for the volume fractions in hybrid composites was presented, and used for the analysis of the experimental data. Good agreement between model predictions and experimental data was observed. Two quantification methods were implemented to analyse the microstructural uniformity of the composites. The methods were demonstrated to be well suitable to quantify the difference in microstructural uniformity between composites, and to detect and quantify any repeating pattern in the composite microstructure.

ACKNOWLEDGEMENTS

This work was conducted in a research project (Blade King, 2008 - 2013) sponsored by the Danish National Advanced Technology Foundation. The authors would like to thank Tom Løgstrup Andersen and Hans Lilholt for valuable advices and support in the manufacturing of composites, and analysis of data.

REFERENCES

Aveston J., Kelly A. (1980). Tensile first cracking strain and strength of hybrid composites and laminates. Phil. Trans. R. Soc. Lond. A, 294: 519-534.

Hermann T.M., Locke J.E. (2006). Fabrication, testing, and analysis of anisotropic carbon/glass hybrid composites. Technical report, Sandia, Lockheed Martin Company, for the United States Department of Energy's National Nuclear Security Administration, USA.

Hillermeier W. (2006). New composite hybrid reinforcements for the wind turbine industry. JEC Composites Magazine. No 49, June 2009.

Zhang J., Chaisombat K., He S., Wang C.H. (2012). Hybrid composite laminates reinforced with glass/carbon woven fabrics for lightweight load bearing structures. Materials and Design, 36: 75-80.